Rough Heston: the *SINC* way

Fabio Baschetti[*]   Giacomo Bormetti[†]   Silvia Romagnoli[‡]

Pietro Rossi[§][¶]

September 2, 2020

Abstract

The goal of this paper is to investigate the method outlined by one of us (PR) in Cherubini et al. (2009) to compute option prices. We named it the SINC approach. While the COS method by Fang and Osterlee (2009) leverages the Fourier-cosine expansion of truncated densities, the SINC approach builds on the Shannon Sampling Theorem revisited for functions with bounded support. We provide several important results which were missing in the early derivation: i) a rigorous proof of the converge of the SINC formula to the correct option price when the support growths and the number of Fourier frequencies increases; ii) ready to implement formulas for put, Cash-or-Nothing, and Asset-or-Nothing options; iii) a systematic comparison with the COS formula in several settings; iv) a numerical challenge against alternative Fast Fourier specifications, such as Carr and Madan (1999) and Lewis (2000); v) an extensive pricing exercise under the rough Heston model of Jaisson and Rosenbaum (2015); vi) formulas to evaluate numerically the moments of a truncated density. The advantages of the SINC approach are numerous. When compared to benchmark methodologies, *SINC* provides the most accurate and fast pricing computation. The method naturally lends itself to price all options in a smile concurrently by means of Fast Fourier

[*]Department of Statistics, University of Bologna, Italy E-mail: fabio.baschetti@studio.unibo.it

[†]Department of Mathematics, University of Bologna, Italy E-mail: giacomo.bormetti@unibo.it

[‡]Department of Statistics, University of Bologna, Italy E-mail: silvia.romagnoli@unibo.it

[§]Prometeia S.p.A., Bologna, Italy E-mail: pietro.rossi@prometeia.it

techniques, boosting fast calibration. Pricing requires to resort only to odd moments in the Fourier space.

Keywords: option pricing; rough Heston model; Fourier expansion; COS method; Fast Fourier methods

1 Introduction

The search of numerically efficient approaches to price options is the subject of intensive research. This fact comes with no surprise, since the ubiquitous presence and crucial role played by contingent claims in modern finance. Without fear of contradiction, it can be affirmed that, when the characteristic function (CF for short) of the log-price process is known in analytic or semi-analytic form, the current standard solution to the pricing problem is the COS method by Fang and Oosterlee (2009). COS – a short-name for Fourier-cosine expansion – builds on the idea that it is computationally convenient to transform the expectation of the payoff with respect to the risk-neutral probability density function (PDF for short) into a linear combination of products of Fourier-cosine coefficients of the payoff and the density. To achieve this goal, one initially pays some price – the key step in the COS development is the approximation of true PDF by a truncated version with bounded support – but this trick eventually reveals to be the crucial step to obtain the best performing pricing formula so far.

Our paper leverages the same idea of truncating the PDF, due to one of us (PR) and outlined in Cherubini et al. (2009), but from a different perspective. It exploits a well-known result which applies to periodic functions with limited bandwidth, i.e. the Shannon Sampling Theorem. The formal symmetry between the forward and backward Fourier transform readily provides the intuition that Shannon's result can be adapted to functions with limited support in the direct space. As an interesting outcome of the application of the Sampling Theorem, one can express Plain Vanilla put and call prices, and digital option constituents, as a Fourier-sinc expansion. Given that the sinc function is the Fourier

transform of the rectangular function, it is not surprising that it may play a crucial role in representing expectations with respect to truncated densities. The convolution between the sinc function – which conveys the information related to the bounded support – and the Fourier transform of the Heaviside step function – which characterizes the point of discontinuity of the digital options – lends itself to analytic simplification by means of Hilbert transforms. As a result, the option price can be represented as a series expansion which only requires the CF computation of the log-price process for odd moments. We refer to this method as *SINC approach*. As an important contribution, in this paper we prove in a rigorous way that the numerical error induced by the PDF truncation and by approximating a double infinite Fourier series by a finite sum can be made arbitrary small.

The need to know the CF in order to apply both COS and *SINC* is in principle a limitation of the approach, which however turns out to be a quite mild drawback. The literature on stochastic models where it is natural to work in the Fourier space is huge and ever growing (see Cherubini et al. (2009) for an overview of the topic). The successful application of Fourier analysis to price options was pioneered by Chen and Scott (1992); Heston (1993); Bates (1996); Bakshi and Chen (1997); Scott (1997). The publication of Duffie et al. (2000) definitely celebrated the role of the transform analysis in dynamic asset pricing models when the state vector follows an affine jump-diffusion. The papers by Carr and Madan (1999) and Lewis (2000, 2001) contributed in a significant way to this stream of research in quantitative finance. In the former, the authors introduced a simple analytic expression for the Fourier transform of the option value, which allows to exploit the considerable computational power of the Fast Fourier Transform (FFT) in the inversion stage. The introduction of FFT techniques boosted the way to real-time calibration, pricing, and hedging. In the latter contributions, Lewis (2000, 2001) detailed a representation of the option price in terms of the CF which is rooted on a clever extension of the Fourier transform in the complex domain. His approach is naturally prone to the application of FFT, too. It is often preferred to the Carr and Madan (1999) approach, which requires the introduction of an auxiliary damping parameter. *SINC* is naturally suited for the computation by means of FFT. Then, not only *SINC* is rooted on a parsimonious

representation of the option payoff, which requires to sample the CF at optimal points, but it expresses the payoff as a transform where the log-moneyness is the conjugate variable in the direct space. As a consequence, all options in a smile can be computed concurrently with $O(N \log_2 N)$ complexity, where N is the number of sample points in Fourier space, enhancing the computational advantage of *SINC* with respect to COS.

The stream of research inspired by the general framework introduced in Duffie et al. (2000) is vast. It ranges from models to equity and exchange rate option pricing, to interest rate derivative pricing, credit risk, and systemic risk modeling. We do not try a review of the literature, which will surely result in a deficient list. Instead, we focus on a restricted but stimulating and flourishing field, the modeling of financial volatility for pricing purposes. Nonetheless, the scope of applicability of the *SINC* methodology is wider, as it will become soon clear. The main reason of the interest in volatility modeling is that, recently, the celebrated Heston model has been revisited in several respects. Jaisson et al. (2015) showed that the Hawkes-based (Hawkes, 1971a,b) market microstructure model of Bacry et al. (2013) under nearly-unstable conditions [1] converges in law to the Heston model. A modification of the microstructure model more aligned with financial data considers the case of nearly-unstable *heavy tailed* Hawkes processes, that is Hawkes processes with an hyperbolic decaying kernel (Hardiman et al., 2013; Bacry et al., 2016). Under this more realistic setting, Jaisson et al. (2016) proved that the process converges to an integrated fractional diffusion. The most surprising fact of this result is that the persistence observed at high frequency is washed out by the aggregation at longer time scale. The limiting process is very irregular, with a derivative behaving as a fractional Brownian motion with Hurst exponent smaller than 0.5 and close to zero. For this reason, the limiting process is dubbed rough Heston (rHeston for short). Gatheral et al. (2018) demonstrated for a wide range of assets that the historical volatility is rougher than a Brownian motion, and that the empirical moment of order q of the log-volatility increments are consistent with a scaling with Hurst exponent of order 0.1. Similar findings are reported in Bennedsen et al. (2016) under the historical measure, while Livieri et al. (2018) investigated the rough behavior of

---

[1] A Hawkes process is nearly-unstable when the L^1 norm of the regression kernel is almost one.

the implied volatility. Finally, contrary to many stochastic volatility models, the rHeston model is able to reproduce the explosive behavior of the implied at-the-money (ATM) skew observed empirically when the option maturity goes to zero (Bayer et al., 2016; Fukasawa, 2011). Remarkably, El Euch and Rosenbaum (2019) derived a semiclosed formula for the CF of rHeston model. The result combines the convergence in law for Hawkes processes and the integral representation of the CF for multivariate Hawkes processes. The formula is not fully explicit but given in terms of the solution of a fractional Riccati equation; the equation admits a unique continuous solution, whose closed form expression is unknown. To avoid the computational burden arising from the numerical solution of the fractional Riccati equation, in this paper we resort to the Padè approximant of the solution already discussed in Gatheral and Radoicic (2019). As claimed in this paper, the rational approximation provides a very accurate description of the solution, especially for low values of the Hurst exponent H. In empirical investigations, both under the pricing and the historical measures, H is found to be of order 0.05-0.1, thus motivating the use of the rational approximation. An alternative approach is provided by the Adams scheme (Diethelm et al., 2004), possibly combined with a power series expansion and Richardson-Romberg extrapolation (Callegaro et al., 2020). We are currently testing these alternatives but postpone the analysis of their numerical viability in a companion paper. For the moment, we remark that in a calibration exercise it is hard to dispute the computational gain of the rational approximation.

As a second main contribution of our paper, we challenge *SINC* against COS and *FFT-SINC* against Carr and Madan (1999) and Lewis (2000, 2001) approaches computed via FFT. Through extensive pricing under the forward variance specification, we assess the superiority in pricing accuracy of *SINC* with respect to competitors. The comparison is performed keeping the same number N_F of points sampled in the Fourier space equal for all methodologies. We believe this is the most fair way to claim the relative performance of the different algorithms, since the number of times the CF needs to be computed in rHeston represents the most time consuming step in pricing. Under this specification, when *SINC* is

challenged against COS, the superiority of the former is apparent. When the full power of FFT is exploited, the reduction of the numerical complexity of *SINC* vs COS is sizable and dramatic, making *SINC* our preferred choice. As a matter of fact when dealing with the rHeston model, the main computational burden comes from the solution of the fractional Riccati equation needed to get the CF. This part greatly outweights the cost of pricing even a highly populated smile and the burden of using FT is twice as big as that of FFT in our exercise. Very much different is the situation where the CF is known analitically; in that case the advantage of having a natural FFT formulation would be very large.

Last, but not least, as a side result of *SINC* approach, we detail in the Appendix a novel analytical methodology to approximate the moments of a random variable starting from the CF.

The remainder of the paper is organized as follows. In Section 2 we discuss the *SINC* formula and in Section 3 we characterize the numerical error. Then, in Section 4 we review the rHeston model by El Euch and Rosenbaum (2019). Sections 5 and 6 present the numerical results from the pricing exercise by means of the *SINC* and FFT-*SINC* specifications, respectively. Section 7 draws the most relevant conclusions. The Appendix provides technical details.

2 *SINC* at a glance

The *SINC* approach to price options is rooted on the following definition of a Fourier pair

$$g(x) = \bar{\mathcal{F}}[\hat{g}(\omega)] = \int_{\mathbb{R}} e^{-i2\pi x\omega} \hat{g}(\omega)d\omega,$$

$$\hat{g}(\omega) = \mathcal{F}[g(x)] = \int_{\mathbb{R}} e^{+i2\pi x\omega} g(x)dx,$$

where $\bar{\mathcal{F}}$ and $\mathcal{F}$ stand for the forward Fourier operator and the inverse Fourier operator, respectively. Under the assumption of null interest rate and dividend yield, i.e. $r = 0$ and $q = 0$, it exploits the following decomposition of a European put into Cash or Nothing

(CoN hereafter) plus Asset or Nothing (AoN) options, i.e.

$$\mathbb{E}[(K - S_T)^+] = K\mathbb{E}[\mathbb{1}_{\{s_T<k\}}] - S_0\mathbb{E}[e^{s_T}\mathbb{1}_{\{s_T<k\}}], \qquad s_T = \log\left(\frac{S_T}{S_0}\right), \quad k = \log\left(\frac{K}{S_0}\right)$$

(1)

with S_T and K denoting the underlying spot at time T and the exercise price, respectively [2].

We note as $\theta(x)$ the Heaviside step function and recognize that contour integration yields

$$\theta(x) = \bar{\mathcal{F}}[\delta^-(\omega)] = \int e^{-i2\pi\omega x}\delta^-(\omega)d\omega,$$

where $\delta^-(\omega) = \frac{i}{2\pi}\frac{1}{\omega+i\varepsilon}$. In the Appendix (Section A), we recall the derivation of the previous result and clarify the role played by ε.

Therefore, if we write each of the expectations on the rhs of Equation (1) in terms of the PDF of the log-return s_T, $f(s_T)$, and the payoff of the option, we have that

$$\mathbb{E}[\mathbb{1}_{\{s_T<k\}}] = \int f(s_T)\theta(k - s_T)ds_T = \bar{\mathcal{F}}\big[\mathcal{F}[f(k)]\mathcal{F}[\theta(k)]\big] = \bar{\mathcal{F}}[\hat{f}(\omega)\delta^-(\omega)]$$

$$= \frac{i}{2\pi}\int e^{-i2\pi k\omega}\hat{f}(\omega)\frac{1}{\omega+i\varepsilon}d\omega,$$

(2)

and

$$\mathbb{E}[e^{s_T}\mathbb{1}_{\{s_T<k\}}] = \int e^{s_T}f(s_T)\theta(k - s_T)ds_T$$

$$= \frac{i}{2\pi}\int e^{-i2\pi k\omega}\hat{f}\left(\omega - \frac{i}{2\pi}\right)\frac{1}{\omega+i\varepsilon}d\omega$$

(3)

by simple means of the convolution theorem and the definition of a Fourier transform (FT for short).

Observe that a change of measure is implicit in the expectation defining the AoN put, which fact requires that $\mathbb{E}[e^{s_T}] = 1$.

---

[2]The general formula for non zero interest rate and dividend yield is readily recovered by setting $s_T = \log(S_T/S_0) - (r-q)T$ and $k = \log(K/S_0) - (r-q)T$ and reads $\text{Put}(t = 0, S_0) = e^{-qT}S_0\mathbb{E}[(e^k - e^{s_T})^+]$.

For any $\eta > 0$, we can find X_l and X_h for which

$$\left| 1 - \int_{X_l}^{X_h} f(s_T)ds_T \right| < \eta,$$

and the Shannon Sampling Theorem (Shannon, 1949) guarantees that the Fourier transform of the truncated function $f(s_T)\mathbb{1}_{X_l \leq s_T \leq X_h}$ can be fully recovered given a discrete (countable) set of points. In the Appendix (Section B), we show that

$$e^{-i2\pi k\omega}\widehat{f\mathbb{1}_{\{X_l \leq s_T \leq X_h\}}}(\omega) = \sum_{n=-\infty}^{\infty} e^{-i2\pi k\omega_n}\widehat{f\mathbb{1}_{\{X_l \leq s_T \leq X_h\}}}(\omega_n)\mathrm{sinc}[2\pi X_c(\omega - \omega_n)], \quad (4)$$

where $\omega_n = n/(2X_c)$, $X_c = (X_h - X_l)/2$, and the sinc function is defined in the usual way as $\sin(x)/x$ (continuous at zero). The idea is that one can truncate the integration range in such a way that the contribution from the tails of the PDF is negligible, and getting rid of it, one can keep control on the approximation error induced on the option price. This is nothing new in the context of Fourier methods and indeed corresponds to the strategy motivating the COS method by Fang and Oosterlee (2009). One handy rule for determining the bounds of the PDF is suggested in Fang and Oosterlee (2009) which set them as

$$[X_l, X_h] = \left[c_1 - L\sqrt{c_2 + \sqrt{c_4}}, c_1 + L\sqrt{c_2 + \sqrt{c_4}} \right], \quad (5)$$

where c_n tags the n-th cumulant of s_T while the choice of L depends on the particular model one is considering. We stick to such a prescription and in Appendix (Section E) we provide original formulas which allow us to evaluate numerically the moments of the distribution – and the cumulants, of course – whenever they are not directly available in closed form (as it is the case with the rHeston model that we consider in the following sections).

Now, we are in the position to recover both CoN and AoN put prices. Nevertheless, we only keep track of the CoN put for making things concise.[3] We plug Shannon's representation

---

[3] The derivation of the AoN put price is perfectly equivalent to the CoN one. We decide to skip it because going through each steps would not add anything new.

(4) into the CoN Equation (2), straightforwardly writing

$$\mathbb{E}[\mathbb{1}_{\{s_T < k\}}] \simeq \mathbb{E}[\mathbb{1}_{\{s_T < k\}} \mathbb{1}_{\{X_l \le s_T \le X_h\}}] = \frac{i}{2\pi} \sum_{n=-\infty}^{\infty} e^{-i2\pi k \omega_n} \widehat{f \mathbb{1}_{\{X_l \le s_T \le X_h\}}}(\omega_n) \int \frac{\text{sinc}[2\pi X_c(\omega - \omega_n)]}{\omega + i\varepsilon} d\omega$$

(6)

and finally solving the inner integral in the *SINC*-based Modified Hilbert transform $\mathcal{H}^-$.

Definition 1. *The Modified Hilbert transform $\mathcal{H}^-$ of a given function g is the result of a convolution of the distribution $\delta^-(x)$ with the function itself. This formally translates as:*

$$\mathcal{H}^-[g(y)] = \int g(x)\delta^-(y - x)dx = \frac{i}{2\pi} \int \frac{g(x)}{y - x + i\varepsilon} dx.$$

In particular, the Appendix (Section C) proves that

$$\int \frac{\text{sinc}[2\pi X_c(\omega - \omega_n)]}{\omega + i\varepsilon} d\omega = \frac{2\pi}{i} \mathcal{H}^-[\text{sinc}(2\pi X_c \omega_n)] = \frac{1}{2X_c \omega_n}(1 - e^{i2\pi X_c \omega_n}),$$

(7)

which is sufficient to specialize the CoN put as

$$\mathbb{E}[\mathbb{1}_{\{s_T < k\}}] \simeq \frac{i}{2\pi} \sum_{n=-\infty}^{\infty} e^{-i2\pi k \omega_n} \widehat{f \mathbb{1}_{\{X_l \le s_T \le X_h\}}}(\omega_n) \left[-i\pi \mathbb{1}_{n=0} + \frac{1 - (-1)^n}{n} \mathbb{1}_{n \ne 0} \right].$$

An additional approximation is introduced when truncating this last infinite sum to a finite (possibly low) number of terms. The error analysis in the Appendix (Section F) shows that such a series truncation error is very well controlled given a suitable choice of N and X_c, and the price of the CoN option is written accordingly as

$$\mathbb{E}[\mathbb{1}_{\{s_T < k\}}] \simeq \frac{i}{2\pi} \sum_{n=-N/2}^{N/2} e^{-i2\pi k \omega_n} \widehat{f \mathbb{1}_{\{X_l \le s_T \le X_h\}}}(\omega_n) \left[-i\pi \mathbb{1}_{n=0} + \frac{1 - (-1)^n}{n} \mathbb{1}_{n \ne 0} \right].$$

The final formula follows replacing $\widehat{f \mathbb{1}_{\{X_l \le s_T \le X_h\}}}(\omega_n)$ with $\hat{f}(\omega_n)$ – Appendix (Section F) assesses the impact of this approximation too – and recognizing that only the odd moments in the Fourier space are relevant for the computation

$$\mathbb{E}[\mathbb{1}_{\{s_T < k\}}] \simeq \frac{1}{2} + \frac{2}{\pi} \sum_{n=1}^{N/4} \frac{1}{2n - 1} \left[\sin(2\pi k \omega_{2n-1}) \Re[\hat{f}(\omega_{2n-1})] - \cos(2\pi k \omega_{2n-1}) \Im[\hat{f}(\omega_{2n-1})] \right],$$

(8)

9

where $\Re$ and $\Im$ denote the real and imaginary parts, respectively. We show the validity of this final formula in Appendix (Section D), and claim that the AoN option is priced in a very similar way, except that the CF needs to be evaluated for a complex argument, i.e.

$$\mathbb{E}[e^{s_T}\mathbb{1}_{\{s_T<k\}}] \simeq \frac{i}{2\pi}\sum_{n=-N/2}^{N/2} e^{-i2\pi k\omega_n}\hat{f}(\omega_n - \frac{i}{2\pi})\Big[-i\pi\mathbb{1}_{n=0} + \frac{1-(-1)^n}{n}\mathbb{1}_{n\neq0}\Big]$$

$$= \frac{1}{2} + \frac{2}{\pi}\sum_{n=1}^{N/4}\frac{1}{2n-1}\Big[\sin(2\pi k\omega_{2n-1})\Re\big[\hat{f}(\omega_{2n-1} - \frac{i}{2\pi})\big]$$

$$- \cos(2\pi k\omega_{2n-1})\Im\big[\hat{f}(\omega_{2n-1} - \frac{i}{2\pi})\big]\Big]. \quad (9)$$

Remark 1. *Out of the $N+1$ terms that we included in the expansions, only $N/4$ survive. They correspond to the positive odd frequencies.*

Equations (8) and (9) finally guarantee that the put option price in Equation (1) accommodates the following form:

$$\mathbb{E}[(K-S_T)^+] \simeq \frac{1}{2}(K-S_0)$$

$$+ \frac{2}{\pi}\sum_{n=1}^{N/4}\frac{1}{2n-1}\Big[\sin(2\pi k\omega_{2n-1})\Re\big[K\hat{f}(\omega_{2n-1}) - S_0\hat{f}(\omega_{2n-1} - \frac{i}{2\pi})\big]$$

$$- \cos(2\pi k\omega_{2n-1})\Im\big[K\hat{f}(\omega_{2n-1}) - S_0\hat{f}(\omega_{2n-1} - \frac{i}{2\pi})\big]\Big]. \quad (10)$$

Equations (8) - (10) represent the main formulas of this paper. They express CoN, AoN, and Plain Vanilla put options in an extremely simple and compact form.

To ease the interpretation of the results in the numerical sections and the comparison among different benchmark methodologies, we introduce the notation N_F to refer to the number of times the CF needs to be evaluated to compute the option price. For instance, to price a CoN, it is sufficient to sample the CF $N_F = N/4$ times at points ω_{2n-1} ($N/4$ times at shifted points $\omega_{2n-1} - i/(2\pi)$ for the AoN) and to weight them with a suitable imaginary phase and the inverse of the integer odd numbers. The price of the Plain Vanilla put is readily recovered from AoN and CoN, thus by means of $N_F = N/2$ valuations of the CF. In the next sections, we are going to support the computational effectiveness of

10

the *SINC* formulas, by challenging them against the COS ones and showing how the *SINC* approach can be readily adapted to the FFT framework.

2.1 The FFT form of *SINC*

One merit of *SINC* is that it is readily adapted to the stiff structure of the FFT algorithm; the computational speed of the Fast Fourier Transform is crucial for any concrete application within the calibration process and the extension comes with almost no effort in our setting.

Our assumption is to price a discrete grid of strikes $k_m = m\frac{2X_c}{N}, -N/2 \leq m < N/2$ and to fit the remaining points, when needed, by linear interpolation from bucket to bucket.

Digital put prices at the aforementioned vector of strikes are now calculated as follows

$$\mathbb{E}[e^{as_T}\mathbb{1}_{\{s_T<k_m\}}] \simeq \frac{i}{2\pi}\sum_{n=-N/2}^{N/2}e^{-i2\pi k_m\omega_n}\hat{f}\left(\omega_n - a\frac{i}{2\pi}\right)\left[-i\pi\mathbb{1}_{n=0} + \frac{1-(-1)^n}{n}\mathbb{1}_{n\neq0}\right]$$

$$= \frac{i}{2\pi}\sum_{n=0}^{N-1}e^{-i\frac{2\pi}{N}mn}q_n \tag{11}$$

where

$$q_n = \begin{cases} \frac{\pi}{i} & n = 0 \\ \hat{f}(\omega_n - a\frac{i}{2\pi})\frac{1-(-1)^n}{n} & n \in [1, \frac{N}{2}) \\ 0 & n = \frac{N}{2} \\ \hat{f}(\omega_{n-N} - a\frac{i}{2\pi})\frac{1-(-1)^{n-N}}{n-N} & n \in (\frac{N}{2}, N-1] \end{cases} \tag{12}$$

and a takes value 0 or 1 for CoN and AoN options, respectively. Equation (11), taken together with the definition of q_n in (12), expresses the SINC formulas in a form which can be readily computed by means of FFT. The formula for the Plain Vanilla put easily follows as before.

Remark 2. *In spite of the fact that the index n runs from 0 to $N-1$, a closer inspection*

reveals that the computation of q_n only requires the evaluation of the CF at $N/4$ different frequencies. Indeed, all q_n for even n are identically zero.

The described procedure generates prices for CoN and AoN digitals indexed by the strikes $n(2X_C/N)$. To recover the price for different strikes (not belonging to the grid) we perform a linear interpolation. The interpolation error can be reduced by increasing the number of terms in the expansion or resorting to the fractional FFT framework (see for instance Chourdakis (2005)).

3 Error Analysis

An analysis similar to that performed in Fang and Oosterlee (2009) shows that there are three sources of error affecting the SINC formula: the approximation of the true PDF with a truncated density, the replacement of a double infinite sum with a finite sum, and the substitution of the Fourier coefficients for the truncated density with the Fourier transform of the true PDF valued at discrete points. To characterize in a quantitative way the three error components, we proceed as follows.

The error associated to our approach can be written as [4]

$$
\begin{aligned}
\epsilon &= \int f(s_T)\theta(k - s_T)\,ds_T - \frac{1}{2} - \frac{i}{2\pi X_c} \sum_{n=-N/4}^{+N/4} e^{-i2\pi k\omega_{2n-1}} \frac{\hat{f}(\omega_{2n-1})}{\omega_{2n-1}} \\
&= \int f(s_T)\theta(k - s_T)\,ds_T - \int_{-X_c}^{X_c} f(s_T)\theta(k - s_T)\,ds_T \\
&+ \int_{-X_c}^{X_c} f(s_T)\theta(k - s_T)\,ds_T - \frac{1}{2} - \frac{i}{2\pi X_c} \sum_{n=-N/4}^{+N/4} e^{-i2\pi k\omega_{2n-1}} \frac{\hat{f}(\omega_{2n-1})}{\omega_{2n-1}}.
\end{aligned}
$$

Exploiting the fact that

$$
\int_{-X_c}^{X_c} f(s_T)\theta(k - s_T)\,ds_T = \frac{1}{2} + \frac{i}{2\pi X_c} \sum_{-\infty}^{+\infty} e^{-i2\pi k\omega_{2n-1}} \frac{\widehat{f\mathbb{1}_{\{-X_c \le s_T \le X_c\}}}(\omega_{2n-1})}{\omega_{2n-1}},
$$

we can write

$$
\epsilon = \int f(s_T)\theta(k - s_T)\,ds_T - \int_{-X_c}^{X_c} f(s_T)\theta(k - s_T)\,ds_T
$$

---

[4] As done before for the pricing formula, we detail the case for the AoN put options. Similar results for the CoN puts can be readily derived.

$$+ \quad \frac{i}{2\pi X_c} \sum_{-\infty}^{+\infty} e^{-i2\pi k\omega_{2n-1}} \frac{\widehat{f \mathbb{1}_{\{-X_c \leq s_T \leq X_c\}}}(\omega_{2n-1})}{\omega_{2n-1}} - \frac{i}{2\pi X_c} \sum_{n=-N/4}^{+N/4} e^{-i2\pi k\omega_{2n-1}} \frac{\hat{f}(\omega_{2n-1})}{\omega_{2n-1}}$$

$$= \quad \int f(s_T)\theta(k-s_T)\,ds_T - \int_{-X_c}^{X_c} f(s_T)\theta(k-s_T)\,ds_T$$

$$+ \quad \frac{i}{2\pi X_c} \sum_{|n|>N/4} e^{-i2\pi k\omega_{2n-1}} \frac{\widehat{f \mathbb{1}_{\{-X_c \leq s_T \leq X_c\}}}(\omega_{2n-1})}{\omega_{2n-1}}$$

$$+ \quad \frac{i}{2\pi X_c} \sum_{-N/4}^{+N/4} e^{-i2\pi k\omega_{2n-1}} \frac{\widehat{f \mathbb{1}_{\{-X_c \leq s_T \leq X_c\}}}(\omega_{2n-1}) - \hat{f}(\omega_{2n-1})}{\omega_{2n-1}} \,. \tag{13}$$

The PDF truncation error reads

$$\epsilon_1 \doteq \int f(s_T)\theta(k-s_T)\,ds_T - \int_{-X_c}^{X_c} f(s_T)\theta(k-s_T)\,ds_T \,,$$

where we introduce the same notation, ϵ_1, used in Fang and Oosterlee (2009). The second and last components of the error in Equation (13), that we refer to with ϵ_2 and ϵ_3 to conform with the notation in Fang and Oosterlee (2009), are the error contributions due to the truncation of a double infinite Fourier series and the replacement of the Fourier coefficients of the truncated PDF with the Fourier transform of the true PDF, respectively.

Such a decomposition of the overall error is the starting point when proving that the *SINC* price converges to the true option price: technical reasons and assumptions essential for the proof are given in the Appendix (Section F), where we bound the magnitude for each of the components in Equation (13) and conclude that the error can be made arbitrarily small by increasing the number of Fourier modes N and the truncation range $[-X_c, X_c]$.

4   The Rough Heston Model

Ease of transposition to the FFT form makes the *SINC* approach very well suited for calibration, and the present paper wants to show that this is an efficient solution for rough volatility models as well. In particular, we will take the rough Heston model as a reference. We recall it in the following for the readers' convenience.

The (generalized) rough Heston model emerging from El Euch and Rosenbaum (2018) is described by the following equations:

$$dS_t = S_t\sqrt{V_t}\{\rho dB_t + \sqrt{1-\rho^2}dB_t^\perp\},$$

$$V_t = V_0 + \frac{\lambda}{\Gamma(H+\frac{1}{2})}\int_0^t \frac{\theta^0(s)-V_s}{(t-s)^{\frac{1}{2}-H}}ds + \frac{\nu}{\Gamma(H+\frac{1}{2})}\int_0^t \frac{\sqrt{V_s}}{(t-s)^{\frac{1}{2}-H}}dB_s,$$

where V_0, λ, and ν are positive real numbers, $\rho \in [-1,1]$. The deterministic function $\theta^0(t)$ is positive and satisfies few constraints specified in El Euch and Rosenbaum (2018). The coefficient $H \in (0,1/2]$ is shown to govern the smoothness of the volatility, whose trajectories enjoy Hölder continuity $H - \epsilon$ for any $\epsilon > 0$. It is therefore clear that the choice $H < 1/2$ allows for a rough behavior of the volatility process and the case $H = 1/2$ amounts to the classical Heston model with time-dependent mean reversion level.

El Euch and Rosenbaum (2018) proved also that the product $\lambda\theta^0(\cdot)$ is directly inferred from the time-0 forward variance curve $\xi_0(t) = \mathbb{E}[V_t|\mathcal{F}_0] = \mathbb{E}[V_t]$, leading to the following specification of the model for $\lambda \to 0$:

$$dS_t = S_t\sqrt{V_t}\{\rho dB_t + \sqrt{1-\rho^2}dB_t^\perp\},$$

$$V_t = \xi_0(t) + \frac{\nu}{\Gamma(H+\frac{1}{2})}\int_0^t \frac{\sqrt{V_s}}{(t-s)^{\frac{1}{2}-H}}dB_s.$$

Remark 3. *The forward variance curve is easily obtained from the variance swap curve by differentiation (see El Euch et al., 2019) and variance swaps valued as in Fukasawa (2012).*

This is extremely convenient for calibration purposes thanks to the reduced dimensionality of the problem. We will consequently work under this last specification throughout the rest of the paper, thus placing ourselves in the same setting of El Euch et al. (2019).

The forward variance curve is a state variable in the model and it also enters the CF of the asset log-price (see El Euch and Rosenbaum (2018) for further details):

$$\varphi(a,t) = \mathbb{E}\left[\exp\left\{ia\log\left(\frac{S_t}{S_0}\right)\right\}\right] = \exp\left(\int_0^t D^\alpha h(a,t-s)\xi_0(s)ds\right),$$

where $\alpha = H + \frac{1}{2}$, $h(a,t)$ is the unique continuous solution of the fractional Riccati equation

$$D^\alpha h(a,t) = -\frac{1}{2}a(a+i) + ia\rho\nu h(a,t) + \frac{\nu^2}{2}h^2(a,t), \qquad I^{1-\alpha}h(a,0) = 0, \qquad (16)$$

and D^α, $I^{1-\alpha}$ denote the Reimann-Liouville fractional derivative and fractional integral of order α and $1 - \alpha$, respectively [5].

Now, Equation (16) is a rough version of the Riccati ODE which emerges in the classical Heston model with zero mean reversion. Here, the standard derivative is replaced by a fractional one. However, such a small change is not painless: the rHeston Riccati equation has no explicit solution and needs to be approximated using numerical methods which are not really plain. In this paper we are not discussing the general issue of an efficient computation of the CF. More precisely, given any approximation to the CF we want to show that the SINC is a very effective method to perform pricing. We will stick with the rational approximation to the CF of Gatheral and Radoicic (2019) and discuss our results within that contest. A second paper, in preparation, will center around the tricky aspects encountered when trying to compute the CF.

5 *SINC* at work

In this section, we perform numerical tests to assess the accuracy of the *SINC* approach. We price European puts and their digital components separately and span over various maturities and moneynesses. The idea is to compare the *SINC* method with the COS method. This second one is known to be very robust and more accurate than any other

---

[5]The Reimann-Liouville fractional derivative of a function f is defined as

$$D^\alpha f(t) = \frac{1}{\Gamma(1-\alpha)}\frac{d}{dt}\int_0^t (t-s)^{-\alpha}f(s)ds \qquad \alpha \in [0,1),$$

provided that it exists. Similarly the fractional integral, provided that it exists, is given by

$$I^\alpha f(t) = \frac{1}{\Gamma(\alpha)}\int_0^t (t-s)^{\alpha-1}f(s)ds \qquad \alpha \in (0,1].$$

alternative in the literature. It is natural to use it as benchmark. The results we will produce in the following sections show that the *SINC*, for the chosen strikes, maturities, and parameter sets, is almost always better than COS when computing call and put options. Always orders of magnitude better when dealing with digital options. Furthermore, *SINC* enjoys the non negligible advantage to be tailor made for the FFT, while the COS, as we know, does not have a painless transition.

We said our experiments are under the rHeston model, with the specific prescription that the forward variance form of El Euch et al. (2019) is used. Parameters are as follows

$$H = 0.05 \qquad \nu = 0.4 \qquad \rho = -0.65,$$

and the forward variance curve supposed to be flat at $\xi_0(\cdot) = 0.0256$. We consider strikes for all the regions of moneyness, i.e. $K = \{0.80, 1.00, 1.20\}$, at both short and long maturities, i.e. $T = \{0.01, 1\}$.

As for truncation of the PDF, we resort to Equation (5), where the cumulants are given by

$$c_1 = m_1$$
$$c_2 = m_2 - m_1^2$$
$$c_4 = m_4 - 4m_1 m_3 + 6m_1^2 m_2 - 3m_1^4,$$

and the moments have been computed by the techniques explained in the Appendix (Section E) [6]. The object of our study is the accuracy of the methods, at this stage, and we consequently take $L = 100$ in spite of different indications in Fang and Oosterlee (2009). Benchmarks are built by pushing *SINC* and COS at very high precision ($N_F = 2^{20}$) and taking all the digits they have in common - or at most ten if they happen to have more.

Table 1 aggregates CoN and AoN puts and reports maximum absolute errors with respect to the benchmark for both *SINC* and COS at different values of N_F, for $T = 1$. The superiority of the *SINC* method w.r.t. the COS, for digital option is strikingly evident.

---

[6]The numerical results presented in this Section are computed assuming $X_h = -X_l = X_c$. This is equivalent to assume $m_1 = 0$.

	K	N_F				
		256	512	1024	2048	4096
SINC	0.80	4.9272e−03	2.6647e−04	5.5175e−07	$\star$	$\star$
	1.00	1.3679e−02	3.5341e−04	4.5323e−07	$\star$	$\star$
	1.20	2.9669e−03	4.6770e−04	9.2800e−07	$\star$	$\star$
COS	0.80	1.3440e−02	1.1897e−02	4.6170e−03	2.5080e−04	5.1600e−07
	1.00	1.1198e−01	3.3614e−02	1.3558e−02	2.8836e−04	3.0859e−07
	1.20	1.0866e−01	2.2281e−02	2.5574e−03	5.4213e−04	1.0379e−06

Table 1: Maximum absolute errors over the couple (CoN, AoN) for *SINC* and COS at different values of N_F. Benchmarks are as follows: CoN = {0.0746857077, 0.3677803881, 0.9746184153}, AoN = {0.0477997904, 0.3222614106, 0.9673515242} for strikes K = {0.80, 1.00, 1.20} respectively; $T = 1$. Stars ($\star$) mean that the price fully conforms with the benchmark (up to the number of digits of the benchmark itself).

When dealing with put options, the COS method partially catches up the *SINC*. Put, as well as call options, are the difference between two digital options, and this introduces cancellations mildly benefiting the SINC but greatly benefiting the COS method. As a consequence, for put or call options, the performance of the COS is still inferior to the SINC but not in such a striking way as it is for digital options.

We stress that the numbers we will see in the following tables do not depend on the moneyness and only focus on options which are struck at $K = 0.80$ [7]. Table 1 confirms that the convergence to the true option price is much faster for *SINC* than it is for COS, when dealing with digital options, and this is markedly evident in Figure 1. The idea behind these charts is that we take our benchmarks as a reference, compute prices with the two methods by increasing $\log N_F$ of one unit per time and stop when we have reached accuracy

---

[7]The reason for this choice is that the traditional method of Carr and Madan (1999) is known to exhibit pathological behaviors when the option is deep OTM and the maturity very short. On the other hand, the COS is insensible to this and we wish to show that so also is the SINC.

of five significant digits on both the CoN and AoN. Not surprisingly *SINC* meets the target
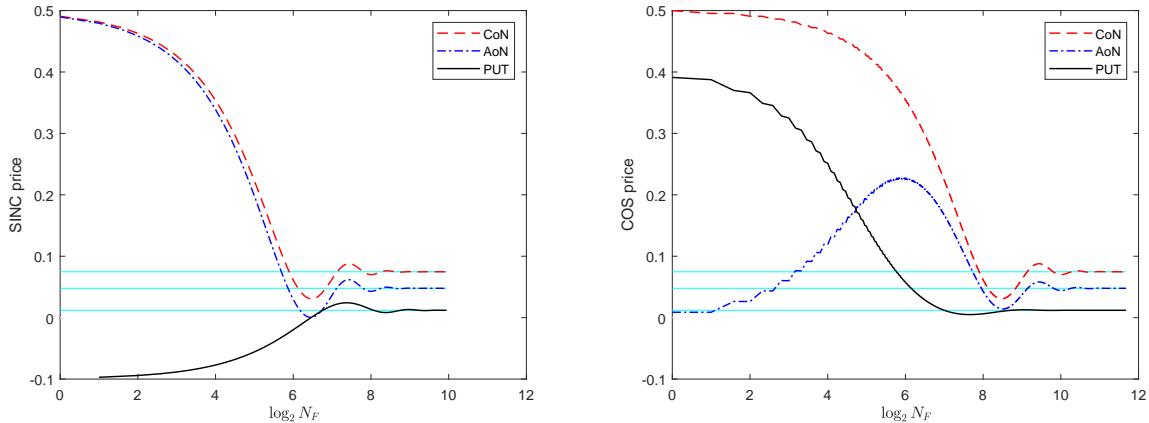

Figure 1: Convergence of the *SINC* (lhs) and the COS (rhs) method. Red (dashed), blue (dot-dashed), and black (bold) lines are the CoN, AoN, and put options, respectively. Light blue horizontal lines denote the benchmarks. $T = 1$ and $K = 0.80$.

for much lower N_F, but we still should recognize that the COS price for the put come closer to the *SINC* performance than its digital components. Note that oscillations last longer on the digital components than the put option itself on the rhs of Figure 1, but they all are less stable than the corresponding *SINC* prices on the lhs of the same Figure.

Before commenting Table 2, it is important to stress a major difference between the *SINC* and COS methods. While COS uses the same frequencies for building the CoN and the AoN, thus computing the CF N_F times for deriving both digital and Plain Vanilla prices, *SINC* uses different frequencies for CoN and AoN. Consequently, it computes put prices by evaluating the CF N_F times, half of them to compute the CoN price and half for the AoN. This is a huge advantage to COS. Nonetheless, the results in Table 2 confirm the superior performance of the *SINC*, where the put option prices for three different strikes, $K = \{0.80, 1.00, 1.20\}$, and maturity $T = 1$ are reported for different values of N_F.

Moreover, we also consider the complex situation where $T = 0.01$. If this seems too short, it is still something one may encounter during the calibration process. It is consequently

		N_F				
	K	256	512	1024	2048	4096
SINC	0.80	1.5951e−03	1.2334e−03	6.5822e−05	1.3886e−07	⋆
	1.00	4.6365e−03	2.1574e−04	6.5050e−05	1.4452e−07	⋆
	1.20	4.9085e−03	1.6262e−04	7.3393e−05	1.1195e−07	⋆
COS	0.80	5.6777e−03	8.3628e−04	4.9324e−05	1.0182e−06	1.1195e−09
	1.00	1.1524e−02	1.6422e−03	9.4302e−05	9.3428e−06	9.7198e−09
	1.20	6.0262e−03	2.4196e−03	2.4696e−04	1.0429e−06	2.0835e−09

Table 2: Maximum absolute errors over put options for *SINC* and COS at different values of N_F. Benchmarks are as follows: put = {0.0119487757, 0.0455189774, 0.2021905741} for strikes $K = \{0.80, 1.00, 1.20\}$, respectively; $T = 1$. Stars ($\star$) mean that the price fully conform with the benchmark (up to the number of digits of the benchmark itself).

useful to understand whether the *SINC* method is robust with respect to pricing options whose expiration is within a couple of days. We only look at the case $K = 0.80$, as usual, and repeat the same analysis as before. The pattern we deduce from Table 3 is very
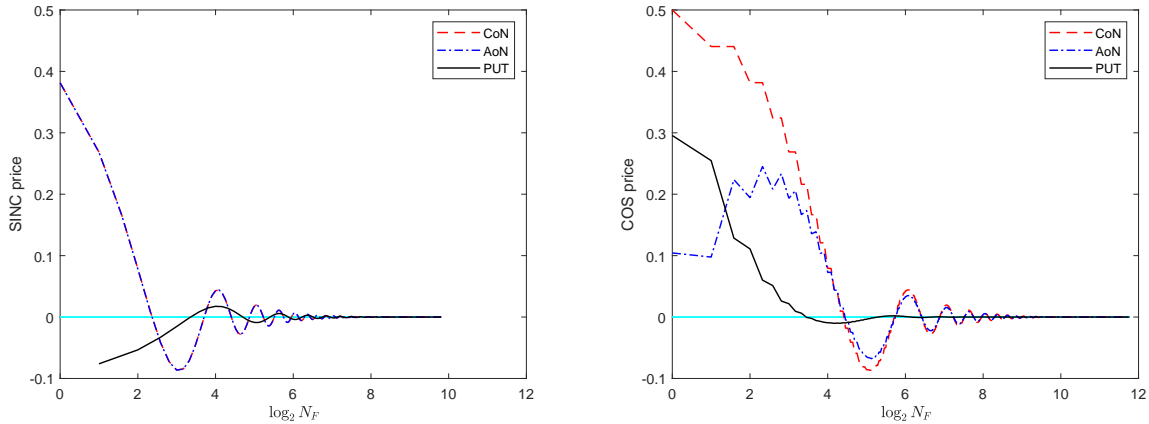

Figure 2: Convergence of *SINC* (lhs) and COS (rhs) method. Red (dashed), blue (dot-dashed), and black (bold) lines are the CoN, AoN, and put options, respectively. Light blue horizontal lines denote the benchmarks $T = 0.01$ and $K = 0.80$.

similar to what we have seen for longer maturities. To ensure fairness, the prices reported

	SINC			COS	
N_F		abs.err.	N_F		abs.err.
256	CoN	——————	256	CoN	——————
	AoN	——————		AoN	——————
	PUT	——————		PUT	——————
512	CoN	6.9486e−07	512	CoN	——————
	AoN	7.2486e−07		AoN	——————
	PUT	——————		PUT	6.6597e−06
1024	CoN	3.6460e−10	1024	CoN	——————
	AoN	3.4810e−10		AoN	——————
	PUT	1.6908e−07		PUT	2.3578e−07
2048	CoN	⋆	2048	CoN	6.9047e−07
	AoN	⋆		AoN	5.4947e−07
	PUT	1.5642e−10		PUT	2.8114e−09
4096	CoN	⋆	4096	CoN	3.6300e−10
	AoN	⋆		AoN	2.7180e−10
	PUT	⋆		PUT	⋆

Table 3: Absolute errors for *SINC* and COS at different values of N_F for $T = 0.01$ and $K = 0.80$. Benchmarks are as follows: CoN = 2.42220e−05, AoN = 1.88150e−05, put = 5.625e−07. Stars ($\star$) mean that the price fully conform with the benchmark (up to the number of digits of the benchmark itself). Horizontal lines mean that the number returned by the algorithm is not meaningful (negative or indistinguishable from zero.)

on each line are computed by means of the same number of sampled frequencies (specified in the N_F columns), independently on the approach. It is worth to notice that for $N_F = 256$ neither *SINC* nor COS provide meaningful values. We need larger values of N_F to reach satisfactory accuracy, but this is an obvious consequence of the much more peaked feature of the PDF implying more difficulties to approximate it in a series expansion (see Figure 3). For $N_F = 512$, apparently only COS is capable to provide a sensible

number. However, it is important to stress that the error (6.6597e−06) is ten times larger than the benchmark values (5.625e−07) rendering the COS value useless. Starting from $N_F = 1024$, both methodologies provide sensible values but the accuracy of the $SINC$ is superior. Figure 2 confirms that $SINC$ prices converge well before the COS counterpart, for digital options, while for Plain Vanilla the gap between the two methods is less marked.
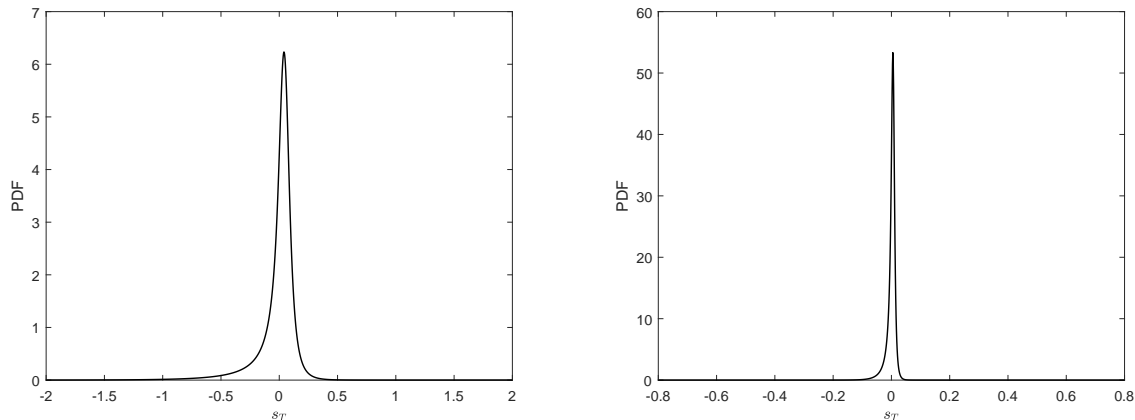

Figure 3: PDF of the asset log-price in the rough Heston model for $T = 1$ (lhs) and $T = 0.01$ (rhs). $H = 0.05$, $\nu = 0.4$, and $\rho = -0.65$.

So if the $SINC$ method is at least as accurate and more efficient than COS - in the sense that convergence to the true option price is generally faster - it is also evident from our explorations that it is very robust with respect to the option's specifics.

We finally want to give one reason to not strictly follow the prescriptions in Fang and Oosterlee (2009) and set $L = 100$ in Equation 5. In fact, it turns out that strict bounds as they suggest (they set $L = 10$) end up with cutting regions of the PDF in the rHeston model whose contribution is not negligible. In Table 4, we quote the absolute differences from the benchmark for a couple of options whose price is computed using a smaller support ($L = 10$) for the PDF of the asset log-return. Even though, apparently, COS is more accurate, indeed the benchmark price is never reproduced. This is going to result in larger errors where one prices indexes whose forward price is thousands of times greater than what we have here.

			CoN	AoN	PUT
$T=1$	$K=0.80$	SINC	4.5248e−07	2.1203e−08	3.4072e−07
$T=1$	$K=0.80$	COS	2.4376e−09	5.1893e−09	3.1792e−09
$T=0.01$	$K=1$	SINC	2.0305e−07	1.3157e−07	7.1488e−08
$T=0.01$	$K=1$	COS	1.4036e−10	1.1111e−08	1.1252e−08

Table 4: Absolute differences from the benchmark which arise when lowering $L = 10$ in Equation 5.

We actually do that with entire surfaces in the next section: for some of the smiles under study, the value of $L = 10$, suggested by Fang and Oosterlee (2009) is clearly inadequate, while 100 seems to be a good choice everywhere we tested both methods. There might be 'optimal' values somewhere in between 10 and 100. We did not look into that detailed optimization.

6 Accuracy and Efficiency of FFT-*SINC*

One strong merit of the *SINC* approach is that it is easily adapted to the FFT form, this fact is crucial for calibration where several strikes have to be computed simultaneously for any given maturity. While the extension is not immediate with COS, one still can count on other methods that are based on a naive discretization of Lewis integral or Carr-Madan traditional technique. In any case, if the former is known to be very slow when it comes to convergence to the true option price, the latter is not really accurate and very sensitive to the options specifics and its tuning parameters. We therefore wish to show that FFT-*SINC* requires much lower N_F to reach some specified accuracy on the implied volatilities, and it is to be consequently regarded as a benchmark method for calibration.

For these purposes, we now price the same volatility surfaces as in El Euch et al. (2019) using model parameters resulting from their calibration, and report average errors on the implied volatility for each smile. The numbers we quote refer to the lowest N_F needed

to make such an average error on the implied volatility smaller than 10^{-4}, and observe that this is achieved with far more effort on the aforementioned alternatives than it is for FFT-*SINC*. Our benchmark prices are computed as the usual intersection between the high-precision SINC and COS candidates. Implementation details for each of the FFT methods are given in the following:

- FFT-*SINC* is given with a truncation range for the PDF which complies to Equation (5), with $L = 100$;

- for Carr-Madan method we fix the dumping parameter at $\alpha_{CM} = 0.9$ and the upper limit of integration as $a_{CM} = 1500$;

- FFT-Lewis extends the integration range according to the usual rule, with $L = 5000$.

As for the model itself, then, we maintain the forward variance form that we have reported in Section 4. The forward variance curve is estimated as a difference on the variance swap curve, and the fair value of a variance swap computed using the methodologies explained in Fukasawa (2012). An iteration procedure is subsequently performed to match model and market at-the-money volatilities through shifting and scaling.

Calibrated parameters for August 14, 2013 are reported in El Euch et al. (2019):

$$H = 0.1216 \qquad \nu = 0.2910 \qquad \rho = -0.6714.$$

With these numbers we compute put option prices for the entire surface based on the FFT methods above. Table 5 reports average errors on the implied volatility for each of the quoted smiles at the lowest value of N_F that satisfies our prior condition. We readily observe that reaching the desired accuracy is much faster for the FFT-*SINC* than for Carr-Madan method and, even more, for a naive discretization of Lewis integral.

Maturity	FFT-*SINC* $N_F = 2048$	FFT-Lewis $N_F = 262144$	Carr-Madan $N_F = 8192$
0.008214	4.1e−05	2.1e−04	8.0e−04
0.024641	4.4e−05	3.4e−04	2.6e−04

0.043806	6.1e−05	1.3e−04	1.6e−04
0.062971	6.9e−05	7.6e−05	1.2e−04
0.082136	7.6e−05	8.3e−05	9.2e−05
0.104038	6.5e−05	1.2e−04	6.1e−05
0.128679	8.1e−05	1.0e−04	5.8e−05
0.180698	8.1e−05	7.0e−05	3.5e−05
0.257358	9.4e−05	8.2e−05	2.7e−05
0.353183	1.1e−04	2.4e−04	2.6e−05
0.380561	9.8e−05	8.0e−05	1.8e−05
0.429843	1.1e−04	1.6e−04	1.8e−05
0.602327	1.3e−04	1.4e−04	1.1e−05
0.626968	1.4e−04	7.9e−05	9.0e−06
0.851472	1.2e−04	2.8e−04	9.0e−06
0.876112	1.1e−04	9.0e−05	6.0e−06
1.349760	1.4e−04	4.4e−04	3.7e−05
1.426420	1.4e−04	9.5e−05	9.0e−06
2.346338	2.0e−04	2.4e−04	2.0e−04

Table 5: Average error per smile on implied volatilities as of August 14, 2013 at the lowest N_F satisfying the condition that the average error per surface is smaller than one basis point.

Remark 4. *Increasing the accuracy of the FFT-SINC to any other level is immediate by simply using an higher N_F, but the same thing is not trivial with Carr-Madan method in view of the documented problems we listed at the beginning of the section.*

We repeat the same analysis for a second date in El Euch et al. (2019). For May 19, 2017 calibrated parameters are:

$$H = 0.0474 \qquad \nu = 0.4061 \qquad \rho = -0.6710.$$

Table 6 confirms what we have seen for the first surface, thus corroborating our claims for a superior performance of the FFT-*SINC*.

Maturity	FFT-*SINC* $N = 2048$	FFT-Lewis $N = 262144$	Carr-Madan $N = 8192$
0.008214	8.8e−05	9.4e−05	7.3e−04
0.013689	1.1e−04	1.2e−04	4.0e−04
0.019165	7.1e−05	2.5e−04	2.7e−04
0.030116	1.0e−04	1.5e−04	1.9e−04
0.032854	8.4e−05	1.7e−04	1.4e−04
0.038330	9.2e−05	1.4e−04	1.3e−04
0.046543	1.2e−04	1.7e−04	1.5e−04
0.052019	1.2e−04	1.7e−04	1.3e−04
0.057495	1.0e−04	1.4e−04	9.6e−05
0.065708	1.4e−04	1.5e−04	1.1e−04
0.071184	1.5e−04	1.4e−04	1.0e−04
0.076660	8.7e−05	1.9e−04	6.5e−05
0.084873	1.6e−04	1.1e−04	8.4e−05
0.090349	1.6e−04	1.2e−04	8.7e−05
0.095825	1.3e−04	1.0e−04	6.0e−05
0.104038	1.3e−04	1.0e−04	6.5e−05
0.109514	1.7e−04	1.2e−04	7.3e−05
0.114990	1.2e−04	1.8e−04	5.9e−05
0.134155	1.5e−04	1.1e−04	5.3e−05
0.153320	1.6e−04	1.1e−04	4.7e−05
0.172485	1.2e−04	1.2e−04	3.3e−05
0.199863	1.5e−04	1.3e−04	2.8e−05
0.249144	1.2e−04	1.1e−04	2.2e−05
0.284736	1.3e−04	1.1e−04	2.3e−05
0.325804	1.1e−04	1.7e−04	2.2e−05
0.364134	1.0e−04	2.6e−04	2.6e−05
0.451745	1.6e−04	9.7e−05	1.5e−05

0.574949	1.2e−04	2.6e−04	1.3e−05
0.613279	1.7e−04	1.2e−04	1.0e−05
0.670773	1.3e−04	1.7e−04	7.0e−06
0.824093	1.8e−04	1.1e−04	7.0e−06
0.859686	2.1e−04	1.2e−04	8.6e−06
1.073238	1.7e−04	1.2e−04	8.9e−06
1.590691	1.9e−04	1.6e−04	7.5e−05
2.587269	2.6e−04	1.9e−04	4.0e−04

Table 6: Average error per smile on implied volatilities as of May 19, 2017 at the lowest N_F satisfying the condition that the average error per surface is smaller than one basis point.

7   Conclusions

The paper investigates the *SINC* approach when pricing European options. *SINC* is shown to be superior to well-known benchmark methodologies. At variance with COS, it allows for an immediate extension to the FFT form. This fact is essential in any calibration exercise. We therefore claim that *SINC* is a promising approach, regarding both the precision it achieves and its numerical efficiency. The numbers we produce in Sections 5 and 6 leave few space for interpretation. They can be obviously reproduced for any other model whose CF is known in closed or semi-closed form. In this respect, our focus on the rHeston model is motivated by the spurring interest on rough volatility models and it is by no means dictated by any limitation of the *SINC* approach.

The idea behind *SINC* is that one first writes put options as a linear combination of digital Asset-or-Nothing and Cash-or-Nothing options. The expectation defining their values is a convolution between the density of the asset log-return and the payoff function. Then, the convolution theorem for Fourier transforms guarantees that each price can be expressed as the integral over a shifted CF. By approximating the CF of the true density with the CF of a truncated PDF, one can fully exploit the potential of the Shannon Sampling Theorem.

It allows to represent the CF at any point by means of a discrete set of frequencies and express it as a Fourier-sinc expansion. Making use of the closed-form representation of the Modified Hilbert transform of the sinc function one can achieve simple and compact formulas for digital and Plain Vanilla put option prices. Moreover, these formulas lend themself to fast computation by means of FFT. The paper provides a rigorous proof of the converge of the SINC formula to the correct option price when the support growths and the number of Fourier frequencies increases. It also investigates several technical prescriptions, such as the computation of truncation bounds by means of a novel technique to compute the cumulants from the CF or the sensitivity of the option prices to the number N_F of frequencies sampled in the Fourier-space. Through an extensive pricing exercise, it assesses the superior performance of the *SINC* approach with respect to the competitor COS methodology. As far as the FFT specification is concerned, the paper challenges *SINC* against the FFT specification of the Lewis formula and the Carr-Madan approach. In both cases, *SINC* proves to be accurate and robust to option's specification.

References

Bacry, E., S. Delattre, M. Hoffmann, and J.-F. Muzy (2013). Modelling microstructure noise with mutually exciting point processes. *Quantitative Finance 13*(1), 65–77.

Bacry, E., T. Jaisson, and J.-F. Muzy (2016). Estimation of slowly decreasing Hawkes kernels: Application to high-frequency order book dynamics. *Quantitative Finance 16*(8), 1179–1201.

Bakshi, G. S. and Z. Chen (1997). An alternative valuation model for contingent claims. *Journal of Financial Economics 44*(1), 123–165.

Bates, D. S. (1996). Jumps and stochastic volatility: Exchange rate processes implicit in deutsche mark options. *The Review of Financial Studies 9*(1), 69–107.

Bayer, C., P. Friz, and J. Gatheral (2016). Pricing under rough volatility. *Quantitative Finance 16*(6), 887–904.

Bennedsen, M., A. Lunde, and M. S. Pakkanen (2016). Decoupling the short-and long-term behavior of stochastic volatility. *ArXiv preprint arXiv:1610.00332*.

Callegaro, G., M. Grasselli, and G. Pages (2020). Fast hybrid schemes for fractional Riccati equations (rough is not so tough). *Preprint*.

Carr, P. and D. Madan (1999). Option valuation using the fast Fourier transform. *Journal of Computational Finance 2*(4), 61–73.

Chen, R.-R. and L. Scott (1992). Pricing interest rate options in a two-factor Cox–Ingersoll–Ross model of the term structure. *The Review of Financial Studies 5*(4), 613–636.

Cherubini, U., G. Della Lunga, S. Mulinacci, and P. Rossi (2009). *Fourier Transform Methods in Finance*. John Wiley & Sons Inc.

Chourdakis, K. (2005). Option pricing using the fractional FFT. *Journal of Computational Finance 8*(2), 1–18.

Diethelm, K., N. J. Ford, and A. D. Freed (2004). Detailed error analysis for a fractional Adams method. *Numerical algorithms 36*(1), 31–52.

Duffie, D., J. Pan, and K. Singleton (2000). Transform analysis and asset pricing for affine jump-diffusions. *Econometrica 68*(6), 1343–1376.

El Euch, O., J. Gatheral, and M. Rosenbaum (2019). Roughening Heston. *Risk*, 84–89.

El Euch, O. and M. Rosenbaum (2018, 12). Perfect hedging in rough Heston models. *Ann. Appl. Probab. 28*(6), 3813–3856.

El Euch, O. and M. Rosenbaum (2019). The characteristic function of rough Heston models. *Mathematical Finance 29*(1), 3–38.

Fang, F. and C. W. Oosterlee (2009). A novel pricing method for european options based on Fourier-cosine series expansions. *SIAM Journal on Scientific Computing 31*(2), 826–848.

Fukasawa, M. (2011). Asymptotic analysis for stochastic volatility: martingale expansion. *Finance and Stochastics 15*(4), 635–654.

Fukasawa, M. (2012). The normalizing transformation of the implied volatility smile. *Mathematical Finance: An International Journal of Mathematics, Statistics and Financial Economics 22*(4), 753–762.

Gatheral, J., T. Jaisson, and M. Rosenbaum (2018). Volatility is rough. *Quantitative Finance 18*(6), 933–949.

Gatheral, J. and R. Radoicic (2019). Rational approximation of the rough Heston solution. *International Journal of Theoretical and Applied Finance 22*(3), 1950010.

Hardiman, S. J., N. Bercot, and J.-P. Bouchaud (2013). Critical reflexivity in financial markets: a Hawkes process analysis. *The European Physical Journal B 86*(10), 442.

Hawkes, A. G. (1971a). Point spectra of some mutually exciting point processes. *Journal of the Royal Statistical Society: Series B (Methodological) 33*(3), 438–443.

Hawkes, A. G. (1971b). Spectra of some self-exciting and mutually exciting point processes. *Biometrika 58*(1), 83–90.

Heston, S. L. (1993). A closed-form solution for options with stochastic volatility with applications to bond and currency options. *The Review of Financial Studies 6*(2), 327–343.

Jaisson, T., M. Rosenbaum, et al. (2015). Limit theorems for nearly unstable Hawkes processes. *The Annals of Applied Probability 25*(2), 600–631.

Jaisson, T., M. Rosenbaum, et al. (2016). Rough fractional diffusions as scaling limits of nearly unstable heavy tailed Hawkes processes. *The Annals of Applied Probability 26*(5), 2860–2882.

Lewis, A. L. (2000). *Option Valuation Under Stochastic Volatility with Mathematica Code.* Finance Press: Newport Beach.

Lewis, A. L. (2001). A simple option formula for general jump-diffusion and other exponential Lévy processes. *SSRN working paper, http://ssrn.com/abstract=282110.*

Livieri, G., S. Mouti, A. Pallavicini, and M. Rosenbaum (2018). Rough volatility: Evidence from option prices. *IISE transactions 50*(9), 767–776.

Scott, L. O. (1997). Pricing stock options in a jump-diffusion model with stochastic volatility and interest rates: Applications of Fourier inversion methods. *Mathematical Finance 7*(4), 413–426.

Shannon, C. E. (1949). Communication in the presence of noise. *Proceedings of the IRE 37*(1), 10–21.

Appendix

A   Inverse Fourier Transform of the θ Function

Let us look at the distribution δ^- and let us recall the definition

$$\delta^-(\omega) := \frac{i}{2\pi} \frac{1}{\omega + i\varepsilon}.$$

In this appendix we want to show the following result:

$$\theta(x) = \int d\omega\, e^{-i2\pi\omega x} \delta^-(\omega). \tag{17}$$

The term $i\varepsilon$ in the denominator of Equation (17) is nothing but the prescription to follow whenever the integration path runs over a singular point. The integral (17) can be computed remaining on the real axis but moving the singularity on the negative imaginary axis as illustrated in Figure (4). When $x < 0$ we can close the integration contour on the upper
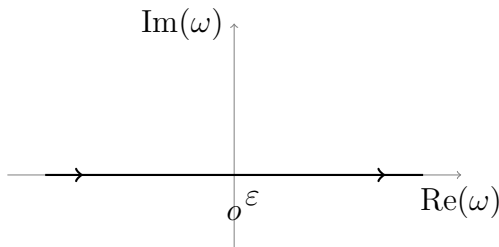

Figure 4: Possible integration path when integrand is $\exp(i2\pi\omega x)/(\omega + i\varepsilon)$.

half plane as in Figure (5) and since there is no pole inside the integration path the result is zero. On the other hand, when $x > 0$ we can close the contour in the lower half plane as in Figure (6). Since we are running clockwise the result will be:

$$
\begin{aligned}
\int d\omega\, e^{-i2\pi\omega x} \delta^-(\omega) &= \frac{i}{2\pi} \int_\Gamma d\omega\, e^{-i2\pi\omega x} \frac{1}{\omega + i\varepsilon} \\
&= \frac{i}{2\pi} \left[-2\pi i e^{-i2\pi\omega(-i\varepsilon)} \right] = 1 \quad x > 0.
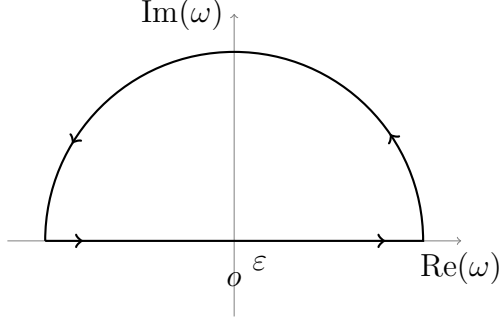\end{aligned}
$$

Figure 5: The integration path when integrand is $\exp(-i2\pi\omega x)/(\omega + i\varepsilon)$ and $x < 0$.
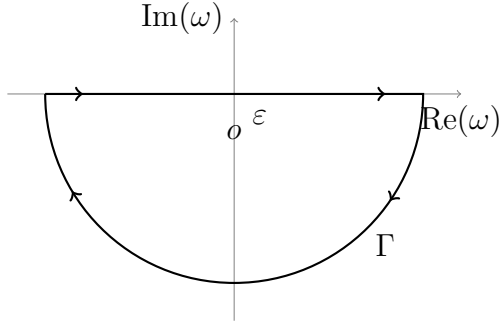

Figure 6: The integration path when integrand is $\exp(-i2\pi\omega x)/(\omega + i\varepsilon)$ and $x < 0$.

B   The Shannon Sampling Theorem

Let us consider a function $c(x)$ whose domain is centered around the origin, i.e. $c(x)$: $[-X_c, X_c] \to \mathbb{R}$. Its Fourier transform is defined as

$$\hat{c}(\omega) = \int_{-X_c}^{X_c} e^{i2\pi\omega x} c(x) dx,$$

and the Fourier Inversion Theorem guarantees that the original function can be written

$$c(x) = \frac{1}{2X_c} \sum_{n=-\infty}^{\infty} \hat{c}(\omega_n) e^{-i2\pi\omega_n x}.$$

An immediate consequence is that

$$\hat{c}(\omega) = \frac{1}{2X_c} \sum_{n=-\infty}^{\infty} \hat{c}(\omega_n) \int_{-X_c}^{X_c} e^{i2\pi(\omega-\omega_n)x} dx = \frac{1}{2X_c} \sum_{n=-\infty}^{\infty} \hat{c}(\omega_n) \frac{e^{i2\pi(\omega-\omega_n)X_c} - e^{-i2\pi(\omega-\omega_n)X_c}}{i2\pi(\omega - \omega_n)}$$

$$= \sum_{n=-\infty}^{\infty} \hat{c}(\omega_n) \frac{\sin[2\pi(\omega - \omega_n)X_c]}{2\pi(\omega - \omega_n)X_c}$$

32

$$= \sum_{n=-\infty}^{\infty} \hat{c}(\omega_n) \mathrm{sinc}[2\pi(\omega - \omega_n)X_c].$$

Similarly, for a function $z(x)$ defined over a bounded interval

$$I_z = \{x : X_l \le x \le X_h\},$$

we get back to the same case as above by properly shifting the function z, i.e.

$$c(x) \doteq z(x + X_m), \qquad X_m = \frac{X_h + X_l}{2}.$$

Hence, knowledge of this next fact

$$\hat{c}(\omega_n) = \int_{-X_c}^{X_c} e^{i2\pi\omega_n x} c(x) dx = e^{-i2\pi\omega_n X_m} \int_{X_l}^{X_h} e^{i2\pi\omega_n x} c(x - X_m) dx = e^{-i2\pi\omega_n X_m} \hat{z}(\omega_n)$$

makes it not difficult to show that

$$\hat{z}(\omega) = \int_{X_l}^{X_h} e^{i2\pi\omega x} z(x) dx = \int_{-X_c}^{X_c} e^{i2\pi\omega(x+X_m)} z(x + X_m) dx$$

$$= e^{i2\pi\omega X_m} \int_{-X_c}^{X_c} e^{i2\pi\omega x} c(x) dx = e^{i2\pi\omega X_m} \hat{c}(\omega)$$

$$= \sum_{n=-\infty}^{\infty} e^{i2\pi\omega X_m} \hat{c}(\omega_n) \mathrm{sinc}[2\pi(\omega - \omega_n)X_c]$$

$$= \sum_{n=-\infty}^{\infty} \hat{z}(\omega_n) \mathrm{sinc}[2\pi(\omega - \omega_n)X_c].$$

C   The Modified Hilbert Transform

The object of our interest are integrals which take the following form

$$\int \frac{\mathrm{sinc}[a(\omega - y)]}{\omega + i\varepsilon} d\omega = \frac{2\pi}{i} \mathcal{H}^-[\mathrm{sinc}(ay)]$$

and their solution based on an application of the Modified Hilbert transform of Definition 1. Then

$$\mathcal{H}^-[\mathrm{sinc}(ay)] = \int \mathrm{sinc}(ax)\delta^-(y - x) dx = \int\int e^{-i2\pi\omega x} \mathcal{F}[\mathrm{sinc}(ax)] d\omega \delta^-(y - x) dx$$

$$= \int \left(\frac{\pi}{|a|} \int e^{-i2\pi\omega x} \mathbb{1}_{[-\frac{|a|}{2\pi} < \omega < \frac{|a|}{2\pi}]} d\omega \right) \delta^-(y - x) dx$$

$$= \frac{\pi}{|a|} \int e^{-i2\pi\omega y} \mathbb{1}_{[-\frac{|a|}{2\pi}<\omega<\frac{|a|}{2\pi}]} d\omega \int e^{+i2\pi\omega(y-x)} \delta^-(y-x) dx$$

$$= \frac{\pi}{|a|} \int e^{-i2\pi\omega y} \theta(-\omega) \mathbb{1}_{[-\frac{|a|}{2\pi}<\omega<\frac{|a|}{2\pi}]} d\omega$$

$$= \frac{\pi}{|a|} \int_{-\frac{|a|}{2\pi}}^{0} e^{-i2\pi\omega y} d\omega = \frac{1}{-2iy|a|}(1 - e^{iy|a|}),$$

where we make use of the fact that the Fourier transform of the sinc function complies to

$$\mathcal{F}[\text{sinc}(ax)] = \int e^{i2\pi\omega x} \frac{\sin(ax)}{ax} dx = \int e^{i2\pi\omega x} \frac{\sin(ax)}{ax - ai\varepsilon} dx = \frac{1}{a} \int e^{i2\pi\omega x} \frac{e^{iax} - e^{-iax}}{2i(x - i\varepsilon)} dx$$

$$= \frac{\pi}{a} \int e^{i2\pi\omega x} \frac{e^{iax} - e^{-iax}}{2\pi i(x - i\varepsilon)} dx = \frac{\pi}{a} \left[\int \frac{e^{i2\pi(\omega+\frac{a}{2\pi})x}}{2\pi i(x - i\varepsilon)} dx - \int \frac{e^{i2\pi(\omega-\frac{a}{2\pi})x}}{2\pi i(x - i\varepsilon)} dx \right]$$

$$= \frac{\pi}{a} \left[\int \frac{i e^{-i2\pi(\omega+\frac{a}{2\pi})x}}{2\pi(x + i\varepsilon)} dx - \int \frac{i e^{-i2\pi(\omega-\frac{a}{2\pi})x}}{2\pi(x + i\varepsilon)} dx \right]$$

$$= \frac{\pi}{a} \left[\theta\left(\omega + \frac{a}{2\pi}\right) - \theta\left(\omega - \frac{a}{2\pi}\right) \right] = \frac{\pi}{|a|} \mathbb{1}_{[-\frac{|a|}{2\pi}<\omega<\frac{|a|}{2\pi}]}.$$

We consequently conclude that our target integral admits solutions of an exponential type

$$\int \frac{\text{sinc}[a(\omega - y)]}{\omega + i\varepsilon} d\omega = \frac{\pi}{y|a|}(1 - e^{iy|a|}),$$

and aptly choosing $a = 2\pi X_c$ and $y = \omega_n$ finally proves the desired result of Equation (7).

D   An Explicit Formulation for the CoN Put Price

This section derives an explicit formulation of the CoN put price, in terms of sin and cos functions multiplying real and imaginary parts of the Fourier transform $\hat{f}$. We have

$$\mathbb{E}[\mathbb{1}_{\{s_T<k\}}] \simeq \frac{i}{2\pi} \sum_{n=-N/2}^{N/2} e^{-i2\pi k\omega_n} \hat{f}(\omega_n) \left[-i\pi \mathbb{1}_{n=0} + \frac{1 - (-1)^n}{n} \mathbb{1}_{n\neq0} \right]$$

$$= \frac{1}{2} + \frac{i}{2\pi} \sum_{n=1}^{N/2} \frac{(1 - (-1)^n)}{n} \left[e^{-i2\pi k\omega_n} \hat{f}(\omega_n) - e^{i2\pi k\omega_n} \hat{f}^\dagger(\omega_n) \right],$$

which can be rewritten as

$$\frac{1}{2} + \frac{i}{\pi} \sum_{n=1}^{N/4} \frac{1}{2n - 1} \left[e^{-i2\pi k\omega_{2n-1}} \hat{f}(\omega_{2n-1}) - e^{i2\pi k\omega_{2n-1}} \hat{f}^\dagger(\omega_{2n-1}) \right].$$

Properly rearranging terms based on Euler's formula, we obtain

$$\frac{1}{2} - \frac{2}{\pi} \sum_{n=1}^{N/4} \frac{1}{2n - 1} \left[\cos(2\pi k\omega_{2n-1}) \Im[\hat{f}(\omega_{2n-1})] - \sin(2\pi k\omega_{2n-1}) \Re[\hat{f}(\omega_{2n-1})] \right].$$

E   Numerical Moments of q-th Order

The computation of the moments of a distribution requires to manage integrals which are not always ensured to admit a closed form solution. Nevertheless, the knowledge of the CF allows to evaluate them numerically. This fact is of crucial importance when truncating the PDF within the *SINC* method but should be clearly recognized to have a much wider scope. That is why we suppress dependence on s_T and talk about a random variable X defined over the support $[-X_c, X_c]$, in this section.

Let us first recall the next fundamental relation between the q-th order moment of X and its CF ϕ_X:

$$\mathbb{E}[X^q] = (i2\pi)^{-q} \frac{\mathrm{d}^q}{\mathrm{d}\omega^q} \phi_X(\omega) \Big|_{\omega=0}$$

then, if we apply the Shannon Sampling Theorem

$$= (i2\pi)^{-q} \sum_{n=-\infty}^{\infty} \phi_X(\omega_n) \frac{\mathrm{d}^q}{\mathrm{d}\omega^q} \mathrm{sinc}(2\pi(\omega - \omega_n)X_c) \Big|_{\omega=0}$$

and perform a simple change of variable, we have

$$= (iX_c)^q \sum_{n=-\infty}^{\infty} \phi_X(\omega_n) \frac{\mathrm{d}^q}{\mathrm{d}t^q} \mathrm{sinc}(t) \Big|_{t=n\pi}. \tag{18}$$

Furthermore, a power series expansion of the sinc function, i.e.

$$\mathrm{sinc}(t) = \sum_{n=0}^{\infty} (-1)^n \frac{t^{2n}}{(2n+1)!}$$

is readily obtained given the corresponding expansion for the sin function, and this clearly justifies a number of properties. Among them we have the following:

1. odd derivatives are such that

$$\frac{\mathrm{d}^{2q+1}}{\mathrm{d}t^{2q+1}} \mathrm{sinc}(t) \Big|_{t=0} = 0$$

by parity of the sinc function

2. terms of the following type

$$\frac{\mathrm{d}^{2q+1}}{\mathrm{d}t^{2q+1}} \mathrm{sinc}(t) \Big|_{t=n\pi}$$

are odd with respect to n

3. even derivatives are such that

$$\left.\frac{\mathrm{d}^{2q}}{\mathrm{d}t^{2q}}\mathrm{sinc}(t)\right|_{t=0} = \frac{(-1)^q}{2q+1}$$

by the theory of Taylor series

4. terms of the following type

$$\left.\frac{\mathrm{d}^{2q}}{\mathrm{d}t^{2q}}\mathrm{sinc}(t)\right|_{t=n\pi}$$

are even with respect to n

These properties play a fundamental role when specifying Equation (18) for some given q. We report the explicit formulation of the first few moments next:

$$
\begin{aligned}
m_1 &= \mathbb{E}[X] = -2X_c \sum_{n=1}^{\infty} \Im\big[\phi_X(\omega_n)\big]\frac{(-1)^n}{n\pi}, \\
m_2 &= \mathbb{E}[X^2] = \frac{X_c^2}{3} + 4X_c^2 \sum_{n=1}^{\infty} \Re\big[\phi_X(\omega_n)\big]\frac{(-1)^n}{(n\pi)^2}, \\
m_3 &= \mathbb{E}[X^3] = -2X_c^3 \sum_{n=1}^{\infty} \Im\big[\phi_X(\omega_n)\big]\left[\frac{(-1)^n}{n\pi}\left(1-\frac{6}{(n\pi)^2}\right)\right], \\
m_4 &= \mathbb{E}[X^4] = \frac{X_c^4}{5} + 8X_c^4 \sum_{n=1}^{\infty} \Re\big[\phi_X(\omega_n)\big]\left[\frac{(-1)^n}{(n\pi)^2}\left(1-\frac{6}{(n\pi)^2}\right)\right].
\end{aligned}
$$

F   Error Analysis (proof)

The overall error ϵ is equal to the sum $\epsilon_1 + \epsilon_2 + \epsilon_3$ and its norm can be bounded as

$$|\epsilon| \leq \epsilon_1 + |\epsilon_2| + |\epsilon_3|.$$

Arguing in the same way as in the COS paper, ϵ_1 can be made arbitrarily small by choosing a sufficiently high value for X_c. As far as ϵ_2 is concerned, it is clear from Equation (6) that it corresponds to the remainder of a series converging to $\mathbb{E}[\mathbb{1}_{\{s_T<k\}}\mathbb{1}_{\{-X_c\leq s_T\leq X_c\}}]$. Then, when N increases, ϵ_2 goes to zero [8].

Concerning ϵ_3, one has

$$|\epsilon_3| \leq \frac{1}{\pi}\sum_{n=-N/4}^{N/4}\frac{1}{|2n-1|}\left|\widehat{f\mathbb{1}_{\{-X_c\leq s_T\leq X_c\}}}(\omega_{2n-1}) - \hat{f}(\omega_{2n-1})\right|.$$

---

[8] It is possible to derive an analytic bound for ϵ_2, assuming some mild regularity for the PDF. The reasoning is similar to that in Fang and Oosterlee (2009).

To bound the last quantity, we can proceed following two strategies, which are based upon different assumptions. We first recall that

$$\hat{f}(\omega_{2n-1}) - \widehat{f\mathbb{1}_{\{-X_c \leq s_T \leq X_c\}}}(\omega_{2n-1}) = \int_{\mathbb{R}\setminus[-X_c,X_c]} f(s_T)e^{i2\pi\omega_{2n-1}s_T}ds_T .$$

To ensure converge of AoN and Plain Vanilla call prices, for $s_T \gg 1$ the PDF $f(s_T)$ has to satisfy

$$f(s_T) \leq Ce^{-\beta s_T} ,$$

with $C > 0$ and $\beta > 1$. For $s_T \ll -1$, we assume the following condition – typically satisfied by commonly used stochastic models for log-returns

$$f(s_T) \leq Ce^{\gamma s_T} ,$$

with $\gamma > 0$. Then,

$$
\begin{aligned}
|\epsilon_3| &\leq \frac{1}{\pi}\sum_{n=-N/4}^{N/4}\frac{1}{|2n-1|}\left|\int_{\mathbb{R}\setminus[-X_c,X_c]}f(s_T)e^{i2\pi\omega_{2n-1}s_T}ds_T\right| \\
&\leq \frac{1}{\pi}\sum_{n=-N/4}^{N/4}\frac{1}{|2n-1|}\int_{\mathbb{R}\setminus[-X_c,X_c]}f(s_T)ds_T \leq \frac{2}{\pi}\sum_{n=0}^{N/4}\frac{1}{2n+1}\int_{\mathbb{R}\setminus[-X_c,X_c]}f(s_T)ds_T \\
&\leq \frac{1}{\pi}(2+\log(N/2+1))\int_{\mathbb{R}\setminus[-X_c,X_c]}f(s_T)ds_T \\
&\leq \frac{C}{\pi}(2+\log(N/2+1))\left(\frac{1}{\gamma}e^{-\gamma X_c}+\frac{1}{\beta}e^{-\beta X_c}\right) .
\end{aligned}
$$

Naming $\delta = \min(\beta,\gamma) > 0$, we obtain

$$|\epsilon_3| \leq \frac{C}{\pi}(2+\log(N/2+1))e^{-\delta X_c} .$$

To conclude, it is sufficient to choose X_c proportional to $\log(N/2+1)$. Practically, this assumption amounts to choose L proportional to $\log(N/2+1)$ in (5). Then, ϵ_3 can be made arbitrarily small by increasing N.

An alternative strategy allows to reach the same conclusion, without assuming the dependence of X_c on N, but under a different hypothesis about the asymptotic behavior of the density $f(s_T)$. We can split the integral $\int_{\mathbb{R}\setminus[-X_c,X_c]}f(s_T)e^{i2\pi\omega_{2n-1}s_T}ds_T$ in two terms, I_1 and I_2, with

$$I_1(\omega_{2n-1}) = \int_{-\infty}^{-X_c}f(s_T)e^{i2\pi\omega_{2n-1}s_T}ds_T \quad\text{and}\quad I_2(\omega_{2n-1}) = \int_{X_c}^{+\infty}f(s_T)e^{i2\pi\omega_{2n-1}s_T}ds_T ,$$

so that

$$|\epsilon_3| \leq \frac{1}{\pi} \sum_{n=1}^{N/4} \frac{1}{2n-1} |I_1(\omega_{2n-1}) + I_2(\omega_{2n-1})| + \frac{1}{\pi} \sum_{n=1}^{N/4} \frac{1}{2n+1} \left| I_1^\dagger(\omega_{2n+1}) + I_2^\dagger(\omega_{2n+1}) \right| . \quad (19)$$

Let us consider $I_2(\omega_{2n-1})$ and define the variable y via the relation

$$s_T = y + \frac{X_c}{2n-1} .$$

Then,

$$
\begin{aligned}
I_2(\omega_{2n-1}) &= -\int_{X_c - X_c/(2n-1)}^{+\infty} e^{i2\pi\omega_{2n-1}y} f\left(y + \frac{X_c}{2n-1}\right) dy \\
&= -\int_{X_c}^{+\infty} e^{i2\pi\omega_{2n-1}y} f\left(y + \frac{X_c}{2n-1}\right) dy - \int_{X_c - X_c/(2n-1)}^{X_c} e^{i2\pi\omega_{2n-1}y} f\left(y + \frac{X_c}{2n-1}\right) dy .
\end{aligned}
$$

It follows that

$$
\begin{aligned}
I_2(\omega_{2n-1}) &= \frac{1}{2} \int_{X_c}^{+\infty} e^{i2\pi\omega_{2n-1}y} \left(f(y) - f\left(y + \frac{X_c}{2n-1}\right) \right) dy \\
&\quad - \frac{1}{2} \int_{X_c - X_c/(2n-1)}^{X_c} e^{i2\pi\omega_{2n-1}y} f\left(y + \frac{X_c}{2n-1}\right) dy
\end{aligned}
$$

so

$$|I_2(\omega_{2n-1})| \leq \frac{1}{2} \int_{X_c}^{+\infty} \left| f(y) - f\left(y + \frac{X_c}{2n-1}\right) \right| dy + \frac{1}{2} \int_{X_c - X_c/(2n-1)}^{X_c} f\left(y + \frac{X_c}{2n-1}\right) dy .$$

We now assume that $f(s_T)$ is monotonically converging to zero for sufficiently large $|s_T|$. The argument of the modulus is positive, so

$$|I_2(\omega_{2n-1})| \leq \frac{1}{2} \int_{X_c}^{X_c\left(1 + \frac{1}{2n-1}\right)} f(s_T)\, ds_T + \frac{1}{2} \int_{X_c}^{X_c\left(1 + \frac{1}{2n-1}\right)} f(s_T)\, ds_T \leq \frac{X_c}{2n-1} f(X_c) .$$

Defining $s_T = y - X_c/(2n-1)$, it readily follows that

$$|I_1(\omega_{2n-1})| \leq \frac{X_c}{2n-1} f(-X_c) .$$

Similar results hold for $I_1^\dagger(\omega_{2n+1})$ and $I_2^\dagger(\omega_{2n+1})$. From Equation (19), we obtain

$$|\epsilon_3| \leq \frac{X_c}{\pi} \left(f(X_c) + f(-X_c) \right) \sum_{n=1}^{N/4} \left(\frac{1}{(2n-1)^2} + \frac{1}{(2n+1)^2} \right)$$

38

$$= \frac{X_c}{\pi} \left(f(X_c) + f(-X_c) \right) \left(\frac{1}{(N/2+1)^2} - 1 + 2 \sum_{n=1}^{N/4} \frac{1}{(2n-1)^2} \right).$$

The partial sum in the last term converges to a positive constant for $N \to +\infty$. So, by expressing $\sum_{n=1}^{N/4}$ as $\sum_{n=1}^{+\infty} - \sum_{n>N/4}$, we can bound $|\epsilon_3|$ as follows

$$|\epsilon_3| \leq \frac{X_c}{\pi} \left(f(X_c) + f(-X_c) \right) \left(\eta - \frac{Q}{N/2+1} + O\left(\frac{1}{(N/2+1)^2} \right) \right),$$

for suitable constants η and Q. By increasing N, the last two terms converge to zero. To conclude, it is sufficient to assume the existence of the first moment of s_T. Indeed, this implies that $f(s_T) = o(1/s_T)$ for $|s_T| \to +\infty$. Then, $X_c f(X_c)$ and $X_c f(-X_c)$ can be made arbitrarily small by choosing X_c sufficiently large.